Wavefield simulations of earthquakes in southern Alaska for tomographic inversion

Vipul Silwal and Carl Tape

Geophysical Institute and Department of Geosciences, University of Alaska Fairbanks

Email: {vsilwal, ctape}@alaska.edu

Overview

We assemble a catalog of moment tensors (Silwal and Tape, 2016) and a three-dimensional seismic velocity model for southern Alaska, in preparation for an iterative tomographic inversion using spectral-element and adjoint methods. The primary geometrical interfaces in the model are the Moho surface, the basement surface of major sedimentary basins, and the topographic surface. The crustal and upper mantle tomographic model is from Eberhart-Phillips et al. (2006), but modified by removing the uppermost slow layer, then embedding the Cook Inlet basin model. We compute 3D synthetic seismograms using the spectral-element method. We demonstrate the accuracy of the initial three-dimensional reference model by comparing 3D synthetics with observed data for several earthquakes originating in the crust and underlying subducting slab. Full waveform similarity between data and synthetics over the period range 5 s to 50 s provides a solid basis for an iterative inversion. The target resolution of the crustal structure is 4 km vertically and 20 km laterally. We use surface wave and body wave measurements from local earthquakes to obtain moment tensors that will be used within our tomographic inversion. Local slab events down to 180 km depth, in additional to pervasive crustal seismicity, should enhance resolution.

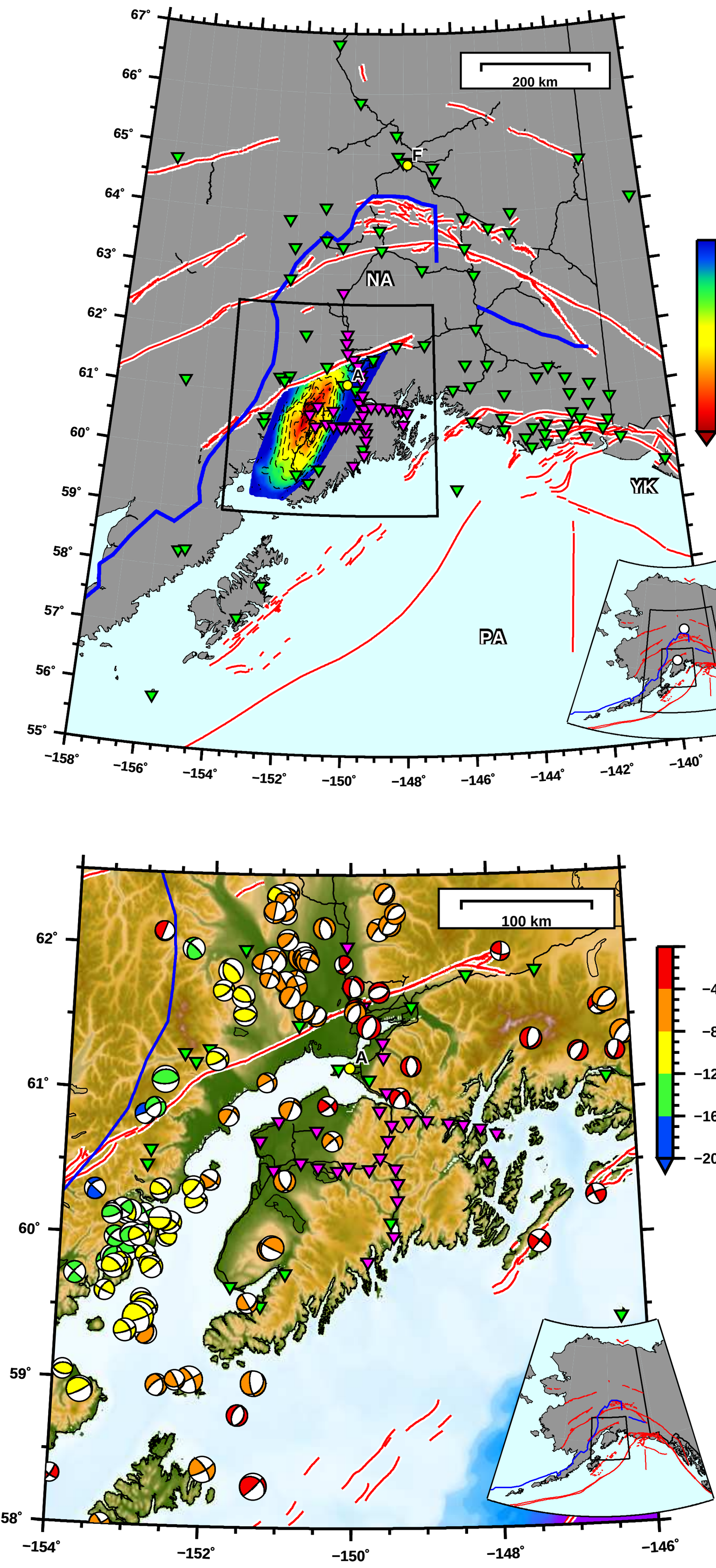

Figure 1: (top) Active faults (red) and the broadband station coverage in Alaska for the time period of this study, 15 August 2007 to 15 August 2009 (green = permanent stations; magenta = MOOS stations). The tertiary basement surface of Cook Inlet basin is color coded for depth. (bottom) Moment tensor beachballs for 106 events presented in the catalog (*Silwal and Tape*, 2016).

Grid search for best moment tensor

We perform a grid search in the moment tensor model space $\mathbf{m} = (\phi, \delta, \lambda, M_w, z)$.

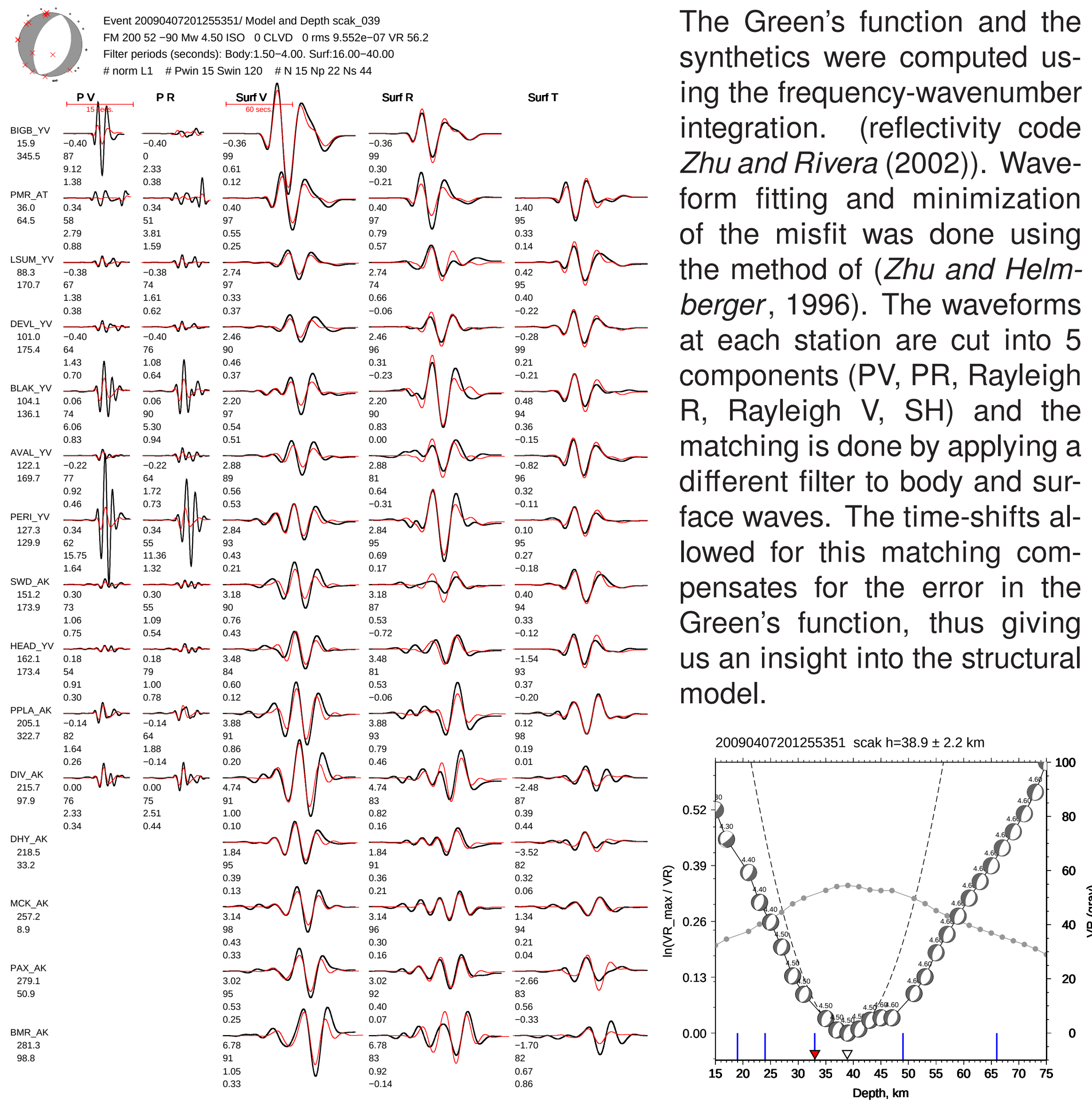

The Green's function and the synthetics were computed using the frequency-wavenumber integration. (reflectivity code *Zhu and Rivera* (2002)). Waveform fitting and minimization of the misfit was done using the method of (*Zhu and Helmberger*, 1996). The waveforms at each station are cut into 5 components (PV, PR, Rayleigh R, Rayleigh V, SH) and the matching is done by applying a different filter to body and surface waves. The time-shifts allowed for this matching compensates for the error in the Green's function, thus giving us an insight into the structural model.

Figure 2: (left) Moment tensor solution and waveform comparisons for the example event in Anchorage, April 7, 2009. Waveform fit between the data (black) and the synthetics (red). Number below the waveforms are, from top to bottom, (1) time shift required for matching the synthetics with the data; (2) maximum cross-correlation percentage between data and synthetics; (3) the percentage of the total misfit; (4) log amplitude between data and synthetics in each window. Number below the station name are distance and azimuth. (right) Grid search for best fitting depth. Blue ticks mark the layer boundaries in the 1D model used in the inversion.

Southern Alaska velocity model

We use 3D velocity model of Alaska obtained from *Eberhart-Phillips et al.* (2006) and embed the Cook Inlet basin model (*Shellenbaum et al.*, 2010) on it. Topography is included in the mesh, and the model is extrapolated wherever necessary. The mesh includes 2 tripling layer at ~8 km and ~50 km. The dimensions of the mesh are: Latitude = [59, 62.5], Longitude = [-154, -147]; and extends to the depth of 400 km. For the 3D adjoint tomographic inversions this will be our starting model.

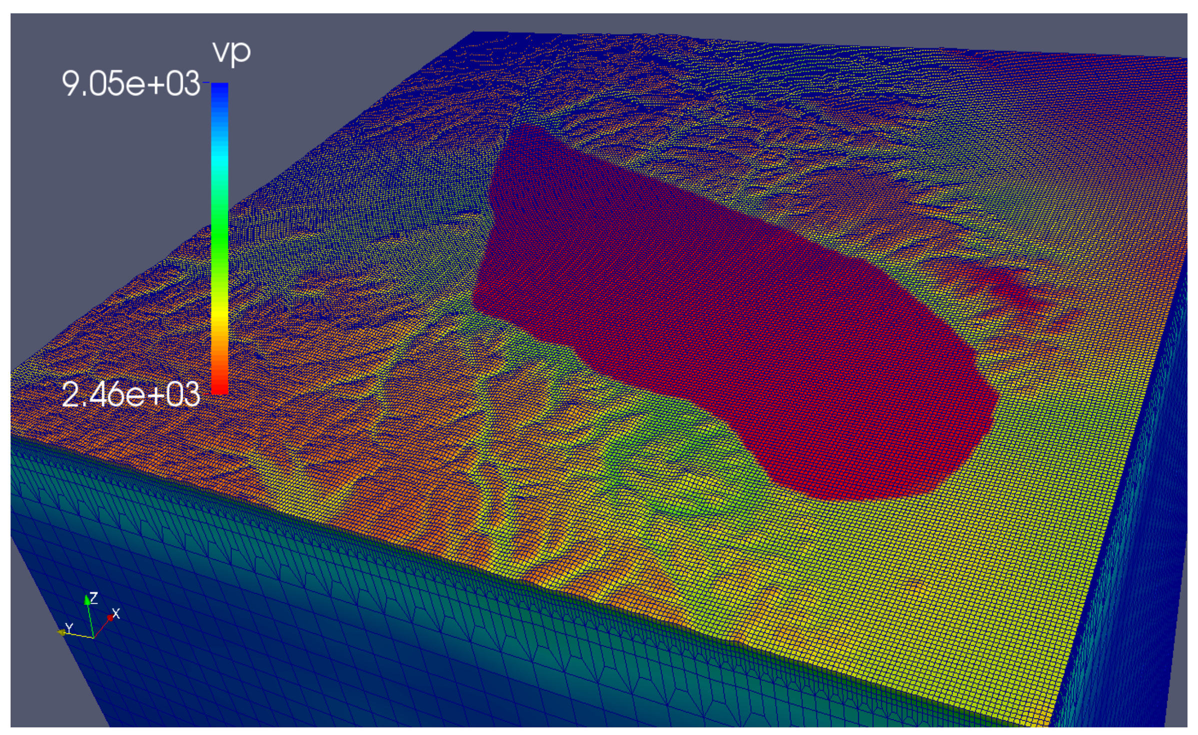

Figure 3: Mesh of southern Alaska with the Eberhart2006 3D velocity model and the Cook Inlet basin (Shellenbaum2010).

Effects of Cook Inlet basin

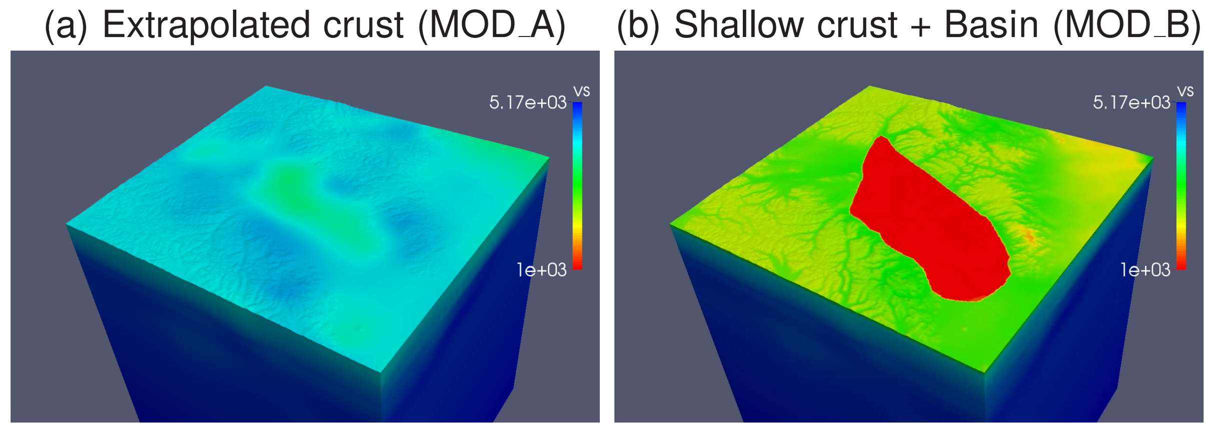

Figure 4: Two different velocity models for studying the effects shallow layers on the waveform. (a) MOD_A - We remove the shallow layer (top 1 km) from the Eberhart2006 model and extrapolate the remaining crustal model upwards. (b) MOD_B - Shallow crustal layer from Eberhart2006 are included and the basin model Shellenbaum2010 has been embedded in it.

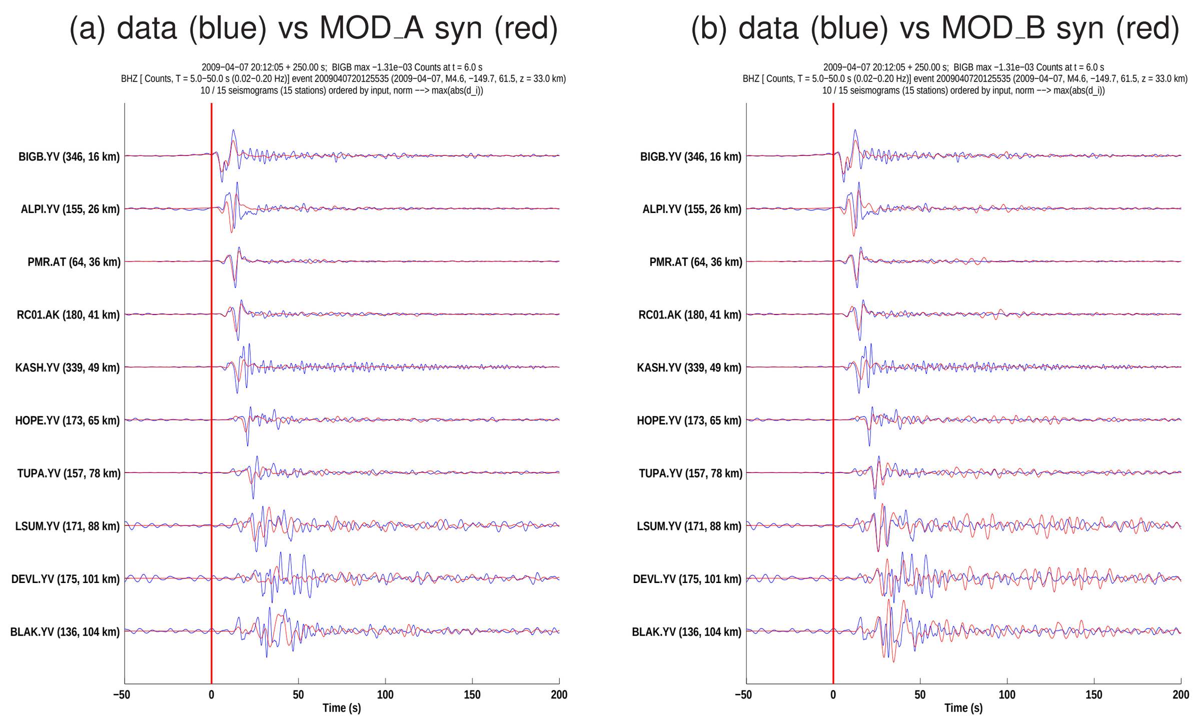

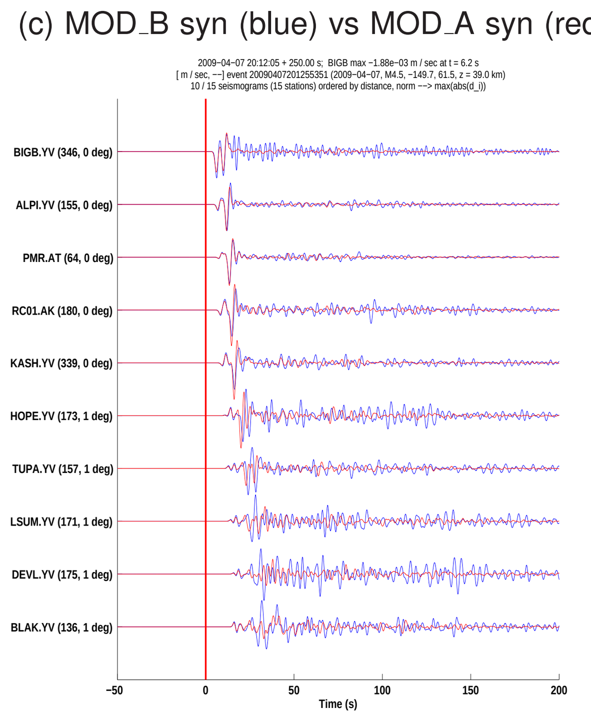

Comparison between waveforms from MOD_A and MOD_B (Figure 4). (a) Comparison between the data (blue) and synthetics (red) when shallow layers are replaced by extrapolated crustal model (MOD_A). (b) Data (blue) vs synthetics (red) when shallow layers and the basin model are included (MOD_B). In both (a) and (b) the waveforms have been filtered between 5–50 s. (c) Comparison between the synthetics from MOD_A and MOD_B. Notice the finer features present in the synthetics when the basin is included. The mesh dimensions were kept same throughout the test and only the velocity model was altered.

Effect of basin on the wavefield

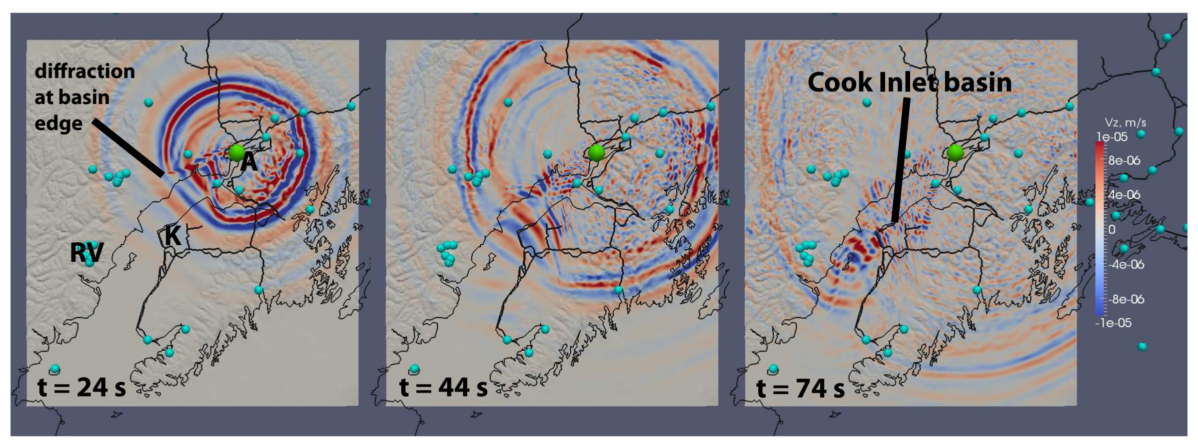

Figure 5: Snapshots of a 3D wavefield simulation of , showing the strong influence of the Cook Inlet basin on the wavefield. Blue circles denote permanent broadband stations. Note the striking effect due to the slow wave speeds within Cook Inlet sedimentary basin. A = Anchorage, K = Kenai, RV = Redoubt volcano.

Simulations of M7.1 Iniskin earthquake

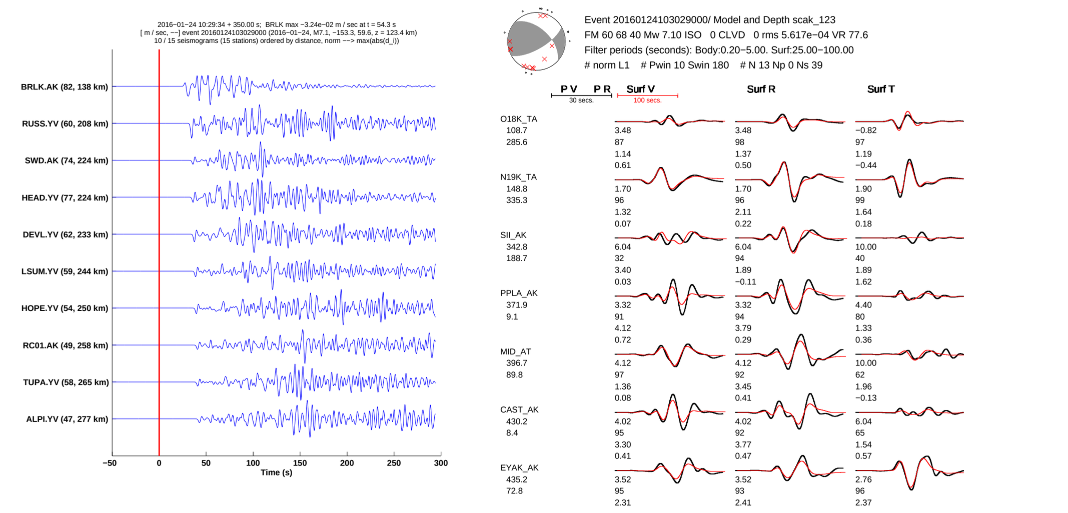

Figure 6: Synthetics for Iniskin earthquake using the 3D velocity model as described earlier (with half duration = 2 sec). (b) The source was estimated using surface waves at 25 - 200 sec generated using 1D SCAK model.

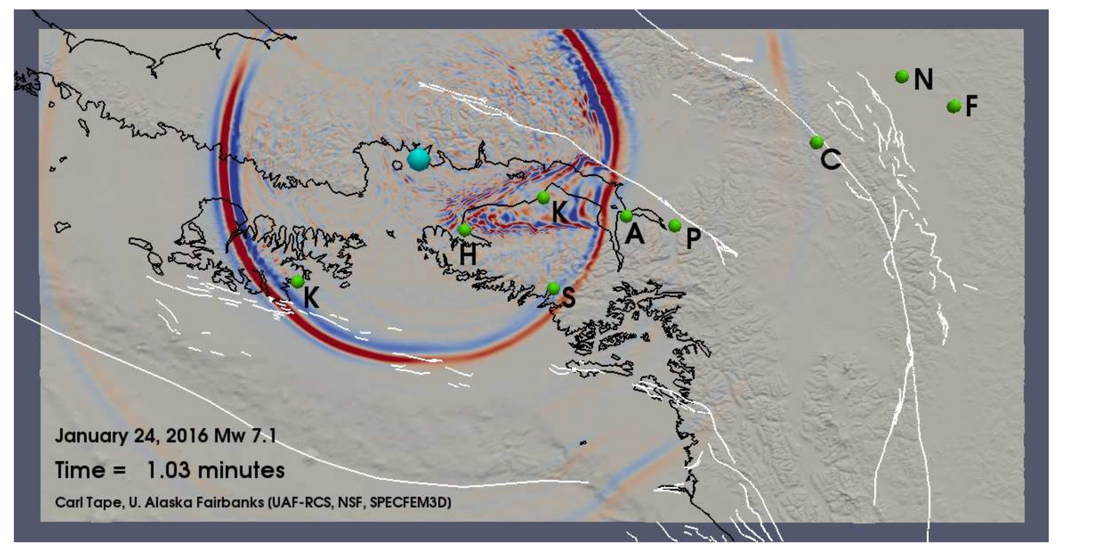

Figure 7: (a) Wavefield simulation of January 24, 2016, M7.1 Iniskin earthquake.
`http://www.giseis.alaska.edu/input/carl/research/earthquakes/iniskin.html`

Summary

1. We perform moment tensor inversions in southern Alaska for 159 earthquakes between 2007-01-01 and 2014-05-01 (*Silwal and Tape*, 2016). The inversions were performed using body waves (1–3 s) and surface waves (16–40 s).
2. Wavefield simulation within a 3D earth structure model produce synthetic seismograms that differ significantly from 1D synthetics but are close enough to observed seismograms to allow us to quantify the waveform misfit and to use these differences within an adjoint tomographic inversion.
3. We examine the influence of the shallowest (slow) layers on 3D synthetic seismograms. It appears that the detailed model for Cook Inlet basin is necessary for achieving reasonable waveform fits, even at relatively long periods (>5 s).
4. Our next step is to calculate 3D synthetic seismograms for all earthquakes, then evaluate a misfit function, then calculate volumetric event kernels to be used within the tomographic inversion, following previous efforts such as in southern California (e.g., *Tape et al.*, 2009).

Acknowledgements

We acknowledge support from NSF grant EAR-1215959. We also appreciate the guidance and suggestions of various members of the CUBIT and SPECFEM community for helping with the occasional breakdowns.

References

Eberhart-Phillips, D., D. H. Christensen, T. M. Brocher, R. Hansen, N. A. Ruppert, P. J. Haeussler, and G. A. Abers (2006), Imaging the transition from Aleutian subduction to Yakutat collision in central Alaska, with local earthquakes and active source data, *J. Geophys. Res.*, *111*, B11303, doi:10.1029/2005JB004240.

Shellenbaum, D. P., L. S. Gregersen, and P. R. Delaney (2010), Top Mesozoic unconformity depth map of the Cook Inlet Basin, Alaska, doi:10.14509/21961, Alaska Div. Geol. Geophys. Surv. Report of Investigation 2010-2, 1 sheet, scale 1:500,000.

Silwal, V., and C. Tape (2016), Seismic moment tensors and estimated uncertainties in southern Alaska, *J. Geophys. Res. Solid Earth*, *121*, 1–26, doi:10.1002/2015JB012588.

Tape, C., Q. Liu, A. Maggi, and J. Tromp (2009), Adjoint tomography of the southern California crust, *Science*, *325*, 988–992, doi:10.1126/science.1175298.

Zhu, L., and D. Helmberger (1996), Advancement in source estimation techniques using broadband regional seismograms, *Bull. Seis. Soc. Am.*, *86*(5), 1634–1641.

Zhu, L., and L. A. Rivera (2002), A note on the dynamic and static displacements from a point source in multilayered media, *Geophys. J. Int.*, *148*, 619–627, doi:10.1046/j.1365-246X.2002.01610.x.